Hindawi
Advances in Materials Science and Engineering
Volume 2022, Article ID 6164599, 10 pages
https://doi.org/10.1155/2022/6164599

Research Article

Improving Sustainability of EDM Sector by Implementing Unconventional Competitive Manufacturing Approach

K. G Sagar,[1] P. K. Anjani,[2] Manju Shree Raman,[3] N. S. M. P. Latha Devi,[4] Kamakshi Mehta,[5] Jose Luis Arias Gonzales,[6] Nellore Manoj Kumar,[7] and Venkatesan S[8]

[1]*Department of Mechanical Engineering, Cambridge Institute of Technology, Bangalore, Karnataka 560036, India*
[2]*Department of Management Studies, Sona College of Technology, Salem, Tamil Nadu 636005, India*
[3]*Department of Management, College of Business & Economics, Debre Tabor University, East Africa, Postal Code: 272, Debre Tabor, Ethiopia*
[4]*Department of Engineering Physics, Koneru Lakshmaiah Education Foundation (KLEF), Vaddeswaram Pincode: 522 302, Guntur, Andhra Pradesh, India*
[5]*Amity College of Commerce, Amity University, Ashiana Angan,Pincode: 301019, Bhiwadi, Haryana, India*
[6]*Department of Business, University of British Columbia, Arequipa, Postal Code: 054, Peru*
[7]*Department of Physics, SCSVMV Deemed Univeristy, Enathur 631561, Kanchipuram, Tamil Nadu, India*
[8]*School of Mechanical Engineering, College of Engineering and Technology, Wachemo University, Hosaena, Ethiopia*

Correspondence should be addressed to Venkatesan S; profsvenkatesan@gmail.com

Received 6 May 2022; Accepted 23 June 2022; Published 11 July 2022

Academic Editor: Pudhupalayam Muthukutti Gopal

In this research work, an attempt was made to machine the titanium (Ti6Al4V) alloy utilizing electric discharge machining technique. The distinct process parameters and its impact on the machining performance were identified using the cause-and-effect diagram (CED). The key process parameters identified by CED diagram were current, pulse on time (Ton), aluminium oxide (Al_2O_3) powder concentration, and gap distance; experiments were conducted by varying the process parameters, experimental runs were designed using the Taguchi mixed orthogonal array. The experimental results revealed that improvement in material removal rate (MRR) was due to the bridging effect; reduction in tool wear rate (TWR) owing to the expansion of spark gap and enhancement in the surface roughness (Ra) was due to the complete flushing of machined debris. The interaction impact was analysed using the contour plot and with the aid of mathematical modelling experimental fits that were identified and the results were validated utilizing the sensitivity analysis. The obtained results were optimized using the technique for order of preference by similarity to ideal solution (TOPSIS) optimization technique.

1. Introduction

The life time of the product depends on the quality of the component used to assemble it. The manufacture of main landing gears from composites using conventional machining processes has distinguishing critical to excellent attributes [1]. The attributes include excessive tool wear due to the presence of abrasive particles in the composites, formation of build-up edges, and exhibiting poor surface as the removal of particles leaves the pits on the surface [2–4]. To resolve this issue, the composites were manufactured using the unconventional machining (UCM) technique, of which electric discharge machining (EDM) was preferred for producing components with utmost quality [5]. The EDM input variable which controls the outcome of the process includes current, spark gap, powder concentration, cycle time, and tool materials [6–8]. Tuning the parameters to the ideal level results in the manufacturing of high-quality items; failing to do so results in faulty products [9]. The route cause for the distinct defects was identified using the CED diagram. The CED, also known

Table 1: Chemical composition of Ti6Al4V (spectrum analysis).

Element	V	Al	Sn	Zr	Mo	C	Si	Fe	Ti
% Composition	4.24	5.48	0.614	0.0031	0.005	0.368	0.03	0.119	89.1409

as the Ishikawa graph or fish-bone investigation, is a directing approach that groups both ordinary and uncommon reasons under the umbrella of the 4M, man machine, methodology, and materials [10]. However, it is possible that the output value y is misled by the set of input quantity ratings (major categories) and other ambiguity elements (subcategories) [11]. There are several instances of CED with jumbled up quantity and uncertainty variables [12].

Current and Ton were the influential parametric setting which influences the machining performance, when the Al_2O_3 was incorporated in the dielectric medium [13]. The shorter Ton results in reduction of Ra value whereas longer current generates heat of high intensity [14]. Hybridisation of machining process enhances the flushing of machined debris and improves the quality of the machined surface [15]. Machined surface property was altered with the changes in the characteristics of dielectric fluid [16]. The optimum duty factor and thermography determine the productivity and quality of titanium alloy [17]. The MRR increased with the increment in the conductivity of the dielectric fluid and over the threshold limit reduces due to upsurge in gap distance [18]. Microcracks were decreased, and the permeability of machined surfaces was improved by suspending a significant quantity of powder at the right proportion [19]. The addition of hydroxyapatite to dielectric fluid changes the discharge gap significantly and affects various input variables as well as dielectric fluid deionization [20].

Selecting best solution from the available alternatives increases the productivity of the industry [21]. Grey relational analysis (GRA), technique for order of preference by similarity to ideal solution (TOPSIS), VIKOR, and multi-objective optimization on the basis of ratio analysis were the distinct optimization technique used for identifying the right parametric combination [22–24]. From the above literature, it was confirmed that the heaps of works were available on the EDM of titanium alloy. However, works related to the machining titanium alloy under Al_2O_3 incorporated dielectric medium were scarcely available. The work was carried out with the following objectives (i) to identify the most influential process parameters through CAD; (ii) to analyse the machining performance by varying the parameters; and (iii) to optimize the process variable through TOPSIS optimization technique.

2. Materials and Methods

Ti6Al4V, a medical grade titanium alloy procured from the Ragavendra Engineering having the chemical composition as depicted in Table 1, was selected for investigation. The process parameters which influence the quality of the manufactured product was identified using the CED. The selected process parameters were varied for four levels, and

Table 2: Input variables and its levels.

Process parameters	Levels
Tool	Cu
Powder concentration (g/l)	5, 10, 15, 20
Polarity	Positive (1), Negative (2)
Pulse ON time (μs)	15
Current (A)	05, 10, 15, 20
Gap distance (mm)	1, 2, 3, 4
Pulse OFF time (μs)	4
Dielectric fluid	EDM oil
Machined time (mins)	10

DOE was designed using the Taguchi orthogonal array as depicted in Table 2. The machining performance was accessed in terms of MRR and TWR, determined according to equations (1) and (2). The Ra was measured utilizing the device SJ210 surface roughness tester, in which the value was computed at 10 different places and the average value was recorded as the Ra value. The copper was used as the electrode, hydro carbon oil as dielectric, and specimens were machined for 10 mins. The results were optimized through TOPSIS technique, a mathematical model was developed, the obtained results were compared with the experimental, and valediction of the model was done through sensitivity analysis.

$$\text{MRR} = \left(\frac{(X_b - X_a)}{z} \right). \tag{1}$$

$$\text{TWR} = \left(\frac{(Y_b - Y_a)}{z} \right). \tag{2}$$

X_b: weight of the work piece before machining
X_a: weight of the work piece after machining
Y_b: weight of the work piece before machining
Y_a: weight of the work piece after machining
z: machined time

The unit of MRR and TWR was mg/min.

2.1. Cause and Effect Diagram. The EDM process parameters were broadly classified into electrical parameters, nonelectrical parameters, electrode parameters, dielectric parameters, powder parameters, and integrated process as shown in Figure 1. The assisted EDM viz. ultrasonic, magnetic was used to facilitate the flushing of the machined debris as well as electrical parameters, gap distance was varied for the same effect, gap distance was picked as one of the input variables keeping the cost in mind. Because dielectric characteristics influence heat generation and changing current results in the same output, several researchers found that current was the

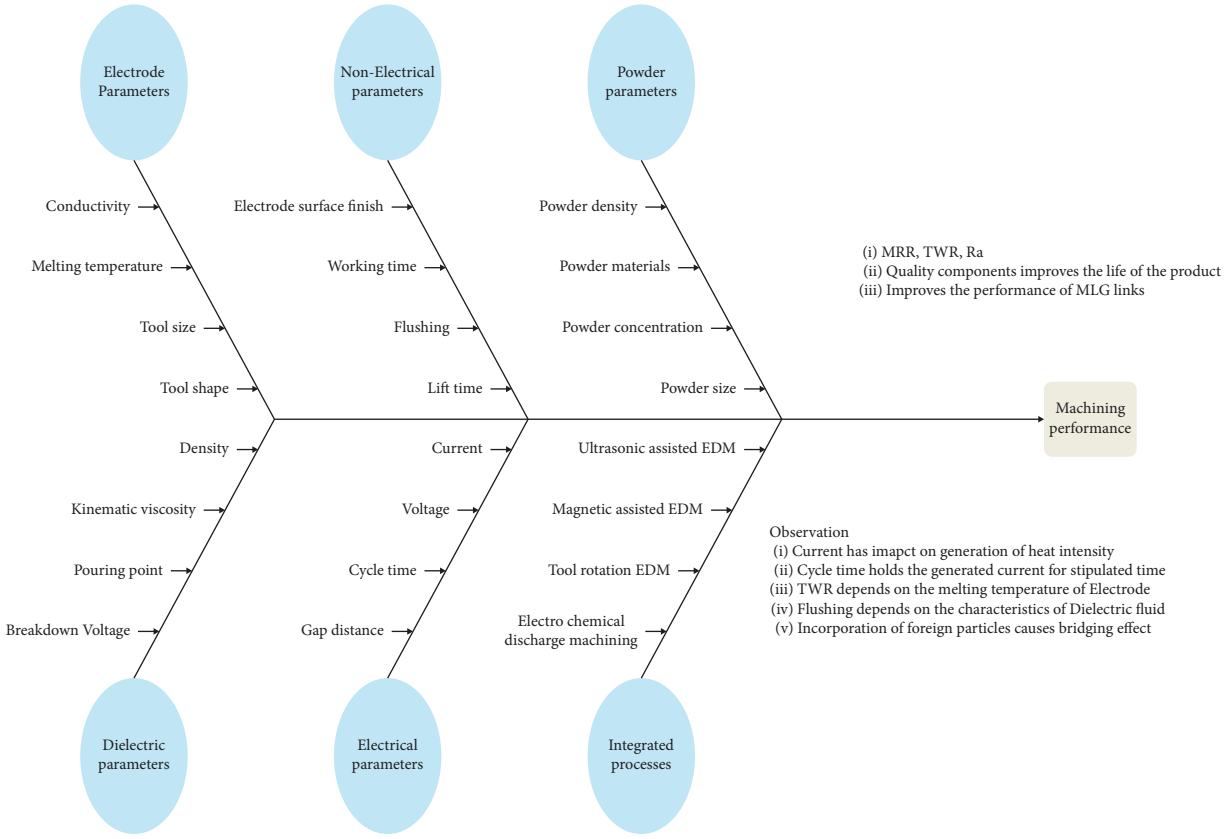

Figure 1: Cause and effect diagram of EDM.

most affecting EDM parameter [25, 26]; hence, current was chosen as the variable. The electrode material characteristics influence the TWR, corner wear, and Ra, whereas change of polarity can yield good surface; hence, these two parameters were selected for investigation.

3. Results and Discussion

3.1. Influence of Distinct Process Parameters on EDM Performance of Ti6Al4V Alloy. Traditionally in EDM, positive polarity was maintained for the effective machining of materials; in special cases, negative polarity was preferred to attain the best Ra value. The MRR of titanium alloy linked to the negative polarity was 18% lower than that of the positive polarity connected electrode as shown in Figure 2; similar result was reported by the distinct researchers [27, 28]. The electrons stream in a straight way and are fit for making secondary electrons while moving to the anode zone and impacting more. It tends to be surmised that the positive polarity zone gets more thermal power than the negative extremity zone. In this way, the emphatically charged anode procures more thermal power than the adversely charged electrode terminal. The MRR upsurges with the raise in concentration of the powder particles in the dielectric fluid; when incorporated with the applied voltage, these particles get energised and travel in a zigzag form. It reduces the spark gap between the electrodes and causes bridging; hence, more heat strucks the work piece, results in the increase in MRR. With the change in current, initially MRR decreases until the 10 A; thereafter, it increases. The reduction in MRR was attributed to the fact that the remove material was remelted over the surface; hence, reduction in volume occurs. The MRR increases with raise in gap distance, as it facilitates the complete flushing of the machined debris.

The interaction effect of various process parameters on the MRR of titanium alloy is shown in Figure 3. When connected to the positive polarity, a maximum MRR of 2.38 mg/min was attained for the current of 15 A and it was reduced to 1.88 mg/min when the polarity was shifted to negative. With regard to the powder concentration, when the volume was 15 g/l at positive polarity, a MRR of 1.59 mg/min was recorded and it was drastically reduced to the 0.82 mg/min, without incorporating powders at negative polarity. The interaction impact of gap voltage and the polarity was very low, as the MRR changes only with the changes in the gap voltage. In case of current and powder concentration, a minimum MRR of 0.86 mg/min was documented at 10 A current under pure dielectric fluid; it was increased to 2.33 mg/min when 20 g/l was added to the fluid at the current of 15 A. Irrespective of the interaction between the gap distance to the either electrical or non-electrical process parameters, MRR varies only with the value of the gap voltage.

The TWR increases with raise in the powder concentration until the saddle point of 5 g/l; thereafter, it declines sharply as shown in Figure 4. The results confirmed that

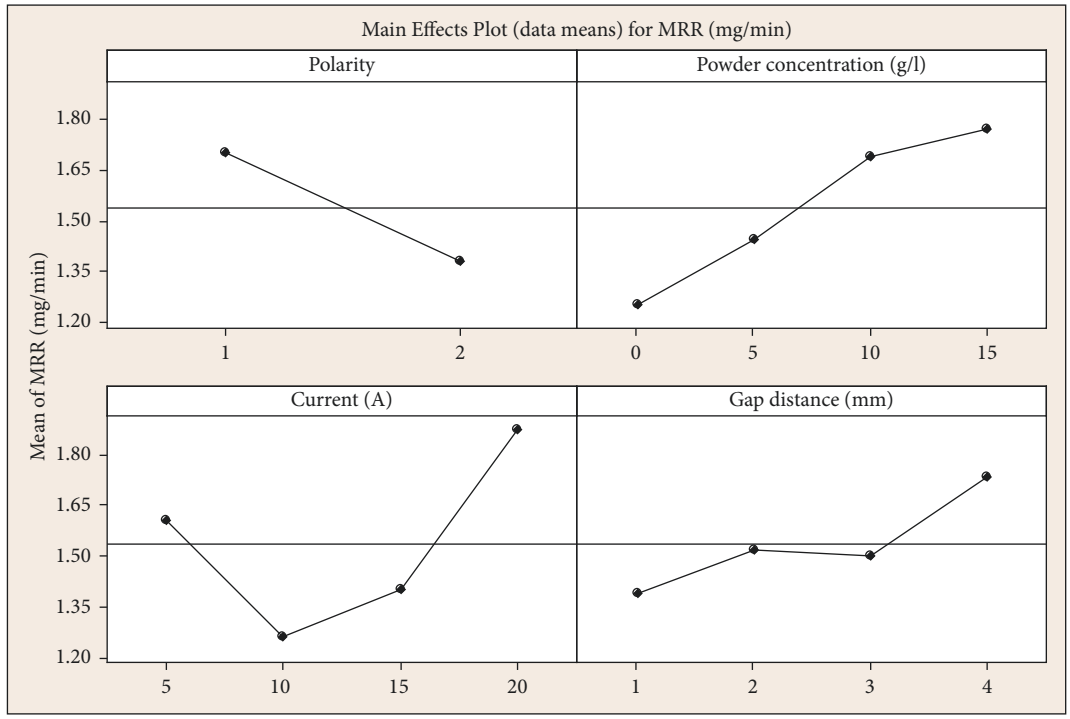

Figure 2: Influence of various process parameters on MRR of Ti6Al4V.

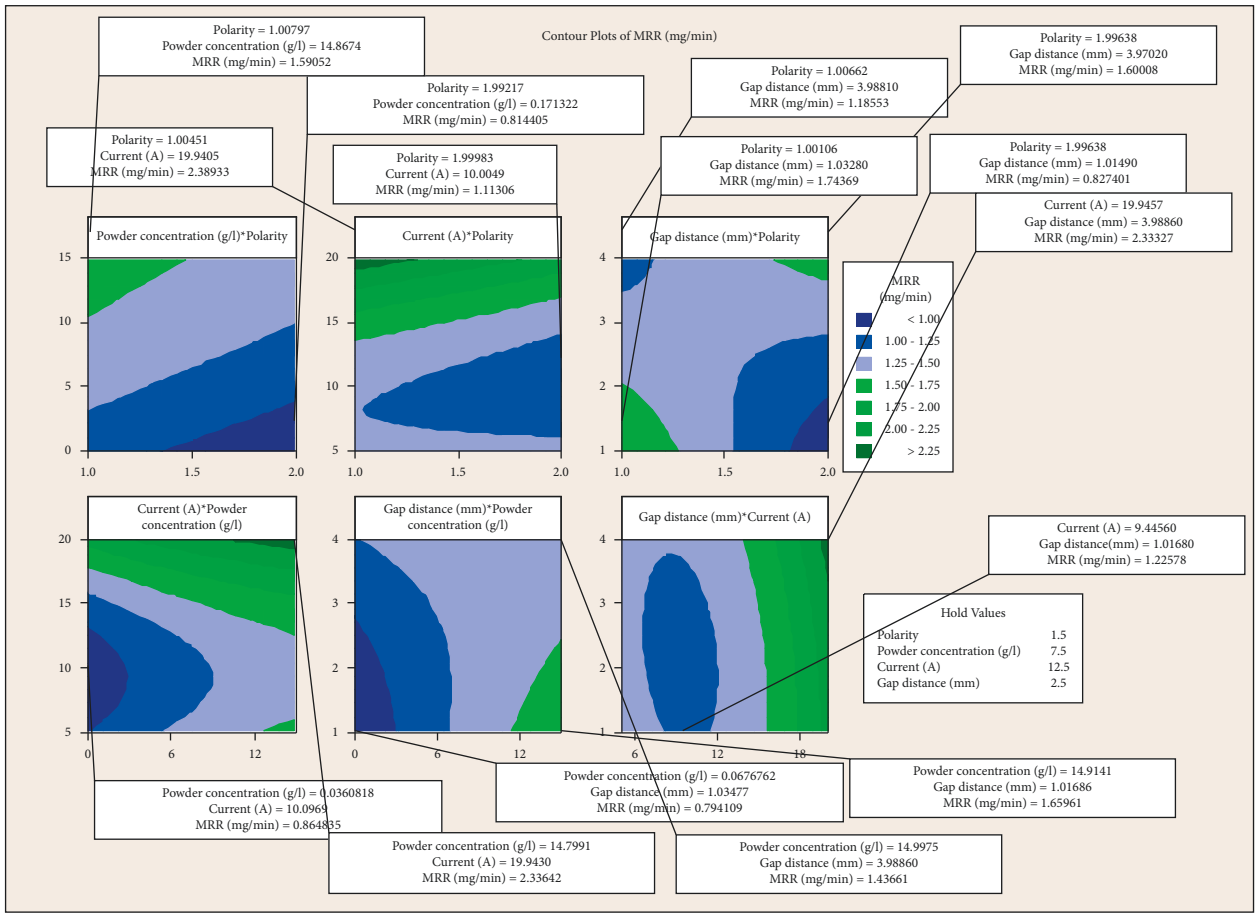

Figure 3: Interaction impact of various process parameters on MRR of Ti6Al4V.

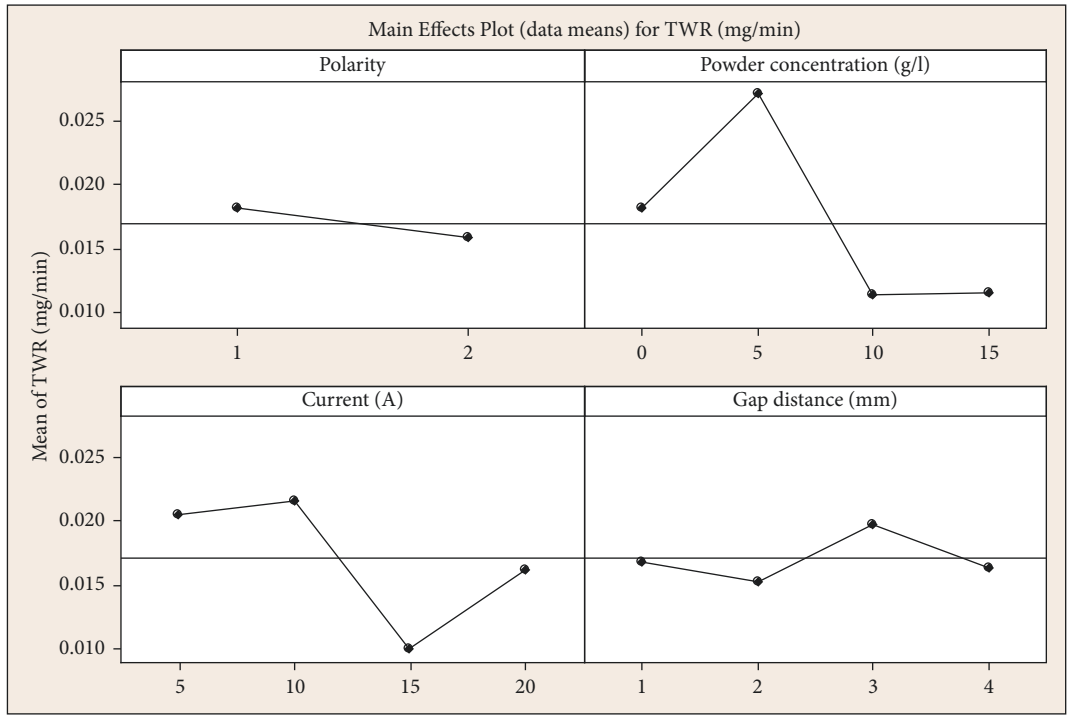

Figure 4: Influence of various process parameters on TWR.

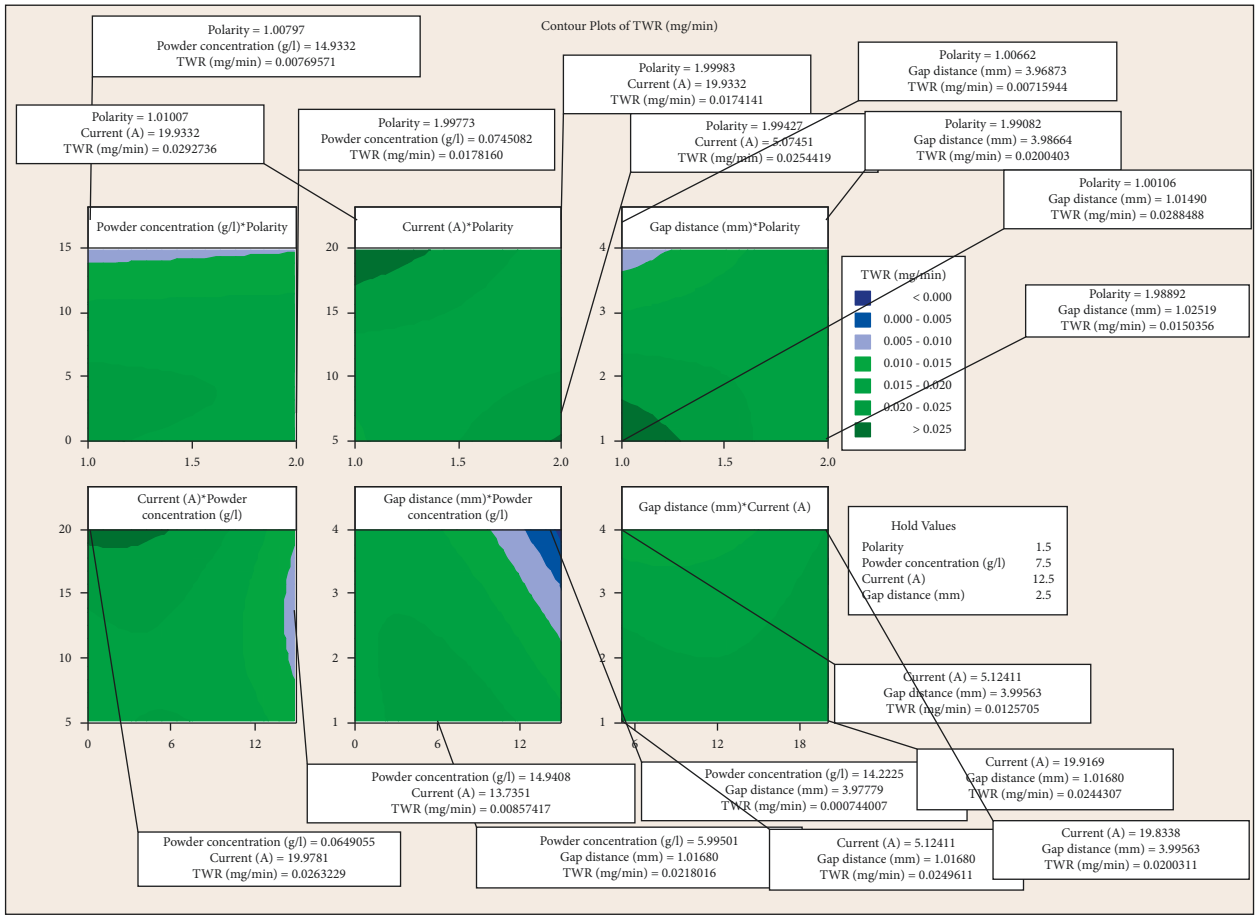

Figure 5: Interaction impact of various process parameters on TWR.

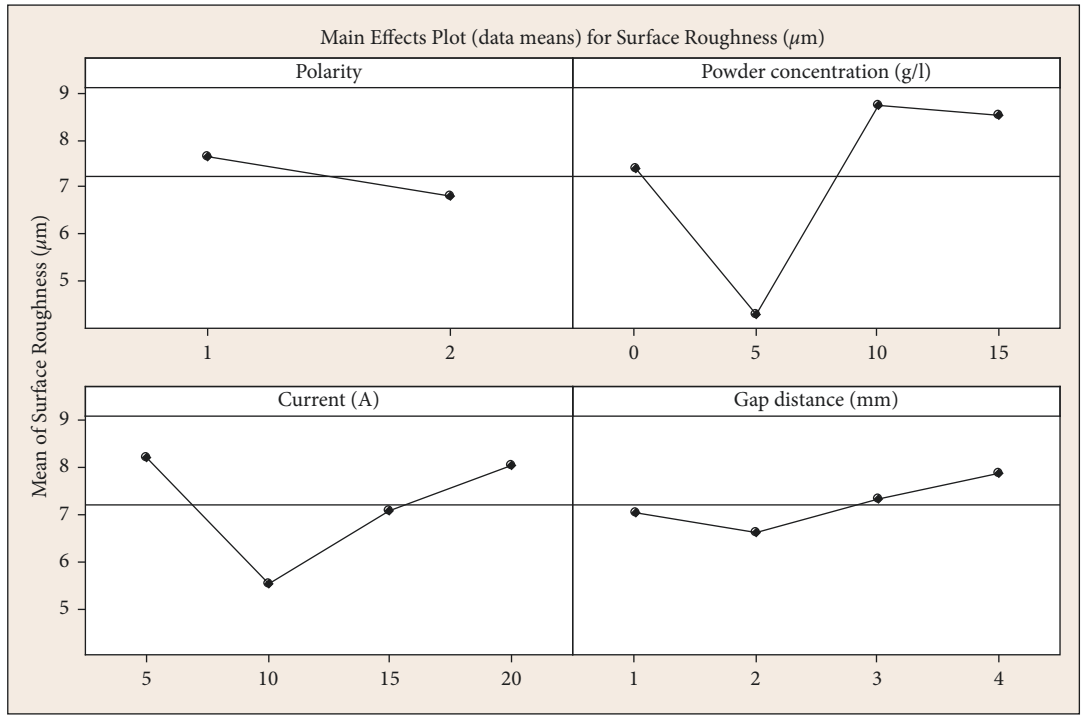

Figure 6: Influence of various process parameters on Ra of Ti6Al4V.

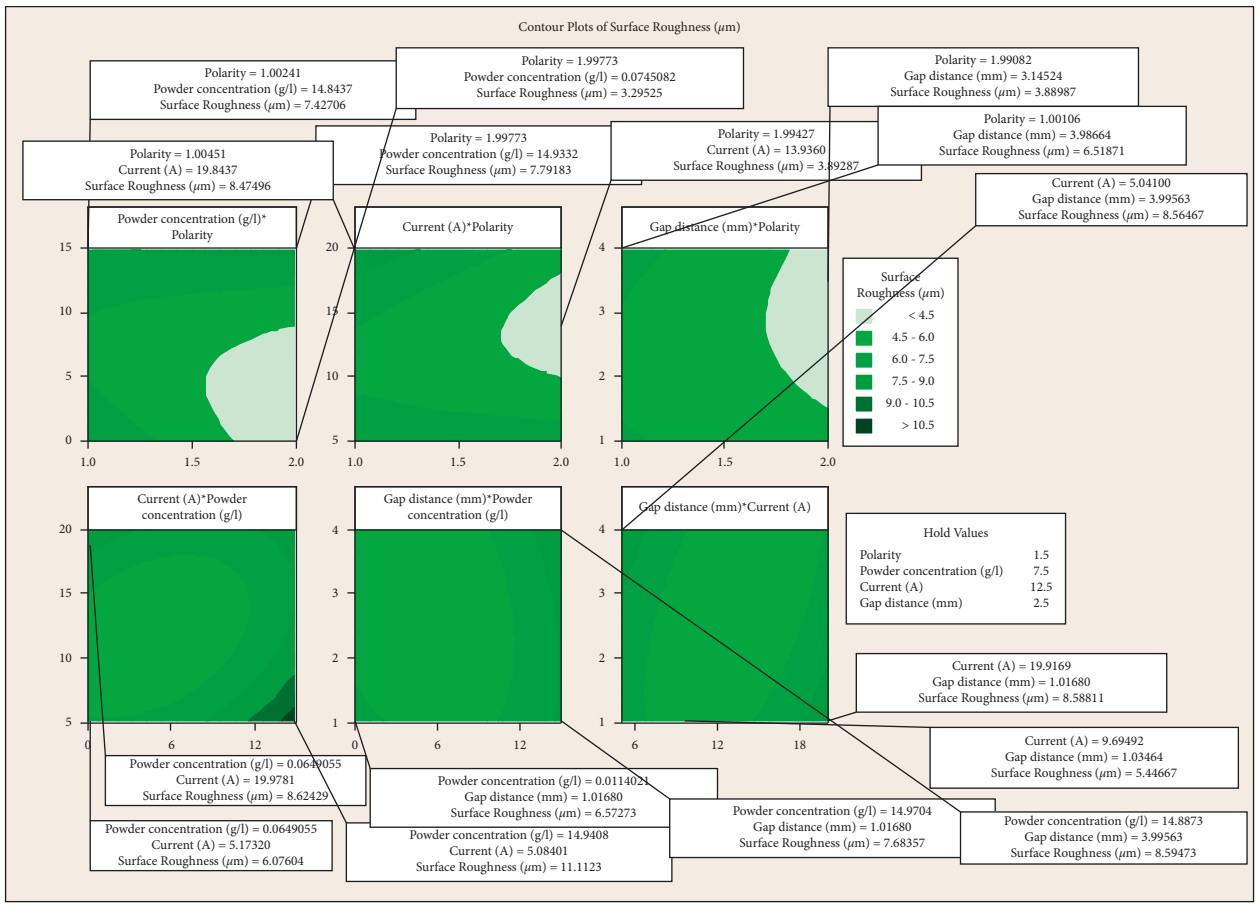

Figure 7: Interaction impact of various process parameters on R_a of Ti6Al4V.

Table 3: Experimental and predicted results of EDM of titanium alloy.

S. No	Polarity	Powder concentration (g/l)	Current (A)	Gap distance (mm)	Experimental results			Predicted results		
					MRR (mg/min)	TWR (mg/min)	Surface roughness (μm)	MRR (mg/min)	TWR (mg/min)	Surface roughness (μm)
1	1	0	5	1	1.12104	0.012881	5.0937	1.26368	0.020663	7.2194
2	1	0	10	2	0.50058	0.030237	5.8203	1.02499	0.01967	6.9701
3	1	0	15	3	1.43855	0.02453	10.1135	1.31362	0.022126	8.0418
4	1	0	20	4	1.96354	0.030574	12.6365	2.12957	0.028032	10.4347
5	1	5	5	1	1.77329	0.035335	8.0071	1.60445	0.025552	6.3456
6	1	5	10	2	1.78704	0.022969	3.7106	1.28392	0.021378	5.7672
7	1	5	15	3	2.01383	0.01143	4.8048	1.49072	0.020655	6.5099
8	1	5	20	4	2.54455	0.026035	4.259	2.22483	0.023381	8.5737
9	1	10	5	2	2.06776	0.001671	9.9741	1.55979	0.01721	7.4412
10	1	10	10	1	1.58518	0.023168	12.2281	1.78501	0.026541	5.9321
11	1	10	15	4	1.31203	0.000234	10.0442	1.45341	0.005816	6.8738
12	1	10	20	3	1.3193	0.014017	5.9908	2.39122	0.022318	8.1542
13	1	15	5	2	0.946	0.016271	8.8559	1.71661	0.01119	9.6801
14	1	15	10	1	2.33251	0.026658	1.6505	2.01041	0.021442	7.2901
15	1	15	15	4	1.44726	0.00321	6.284	1.44657	-0.00656	8.4546
16	1	15	20	3	2.99926	0.01105	13.0695	2.45294	0.010858	8.8541
17	2	0	5	4	1.82468	0.026262	6.1482	1.49891	0.026343	5.4697
18	2	0	10	3	0.44802	0.01432	1.5727	0.93737	0.020672	3.1891
19	2	0	15	2	1.56279	0.004438	5.4497	0.76502	0.014777	4.2318
20	2	0	20	1	1.1429	0.001447	12.2119	0.98187	0.008656	8.5978
21	2	5	5	4	1.48571	0.02871	6.1791	1.64737	0.026629	6.8881
22	2	5	10	3	0.16613	0.039399	1.6682	1.1544	0.021879	3.7265
23	2	5	15	2	1.01663	0.02699	4.2928	1.05062	0.016904	3.8883
24	2	5	20	1	0.7439	0.025968	1.4748	1.33603	0.011704	7.3733
25	2	10	5	3	1.85968	0.030637	9.9594	1.51639	0.024087	8.6801
26	2	10	10	4	1.83308	0.001335	9.1525	1.57665	0.017975	6.2266
27	2	10	15	1	1.14958	0.0049	5.8941	1.08967	0.012393	5.8469
28	2	10	20	2	2.36929	0.015075	6.7705	1.86251	0.013451	6.1829
29	2	15	5	3	1.78266	0.01264	11.7626	1.63131	0.017565	12.6594
30	2	15	10	4	1.46302	0.014237	8.3857	1.60973	0.008273	9.8768
31	2	15	15	1	1.2776	0.003594	9.8181	1.34173	0.007712	8.0643
32	2	15	20	2	1.90664	0.004657	8.2322	2.03273	0.00559	8.0712

when 5 g/l concentration of powder particles was added, most of the generated heat was transferred to the tool materials; hence, TWR increases. With further increase in powder concentration, densification of machined debris occurred, and in case of current, a minimum TWR was obtained at 15 A. The gap distance has predominant impact on the TWR; 20% deviation was observed when there is shift in parametric value from 2 mm to 3 mm. At positive polarity, without mixing particles in the dielectric fluid, a TWR of 0.020 mg/min was observed and it was reduced to 0.017 mg/min when electrodes were connected to negative polarity as depicted in Figure 5. In particle mixed dielectric condition, change in polarity has no impact on the TWR which is evident that incorporation of particles transfers more volume of heat to workpiece [29]. When the current was tuned at lower parametric value, the TWR increases when there is changeover in polarity from positive to negative extreme, and at higher current, TWR reduces with change in polarity. Irrespective of the gap distance, 100% raise in TWR was noted, when electrodes were connected to the positive terminal. The minimum TWR of 0.008 mg/min and 0.007 mg/min was obtained for the current and gap distance of 15 A and 4 mm, respectively, at the powder concentration of 15 g/l.

The impact of various process parameters on the Ra of the Ti6Al4V is depicted in Figure 6. The results showed that sample machined at negative polarity exhibits least Ra, as reported by the various researchers [30, 31]. Attributable to the higher thermal power, the materials eliminated from the cathodes were totally flushed away; henceforth, it dispenses with the formation of remelted layer. As the Ra of the workpiece was impacted by the recast layer, it was evident that the tool extremity influences the Ra of the machined workpiece in EDM process. With regard to the raise in current, a minimum Ra of 5.52 μm was attained; further raise in current worsens the surface quality. At higher current, densification of plasma channel occurred, which results in the formation of material dooms and uneven machined surface; hence, Ra reduces. The best surface quality was attained, when 5 g/l of Al_2O_3 particles were added to the dielectric fluid. When the powder particles were incorporated, owing to the bridging effect, the gap between the tool and electrode increases which facilitates the thorough flushing of machined debris resulting in the reduction of Ra.

Table 4: Assessment values obtained through TOPSIS optimization technique.

Nomalised decision matrix			Weighted normalized decision matrix						
MRR (mg/min)	TWR (mg/min)	Surface roughness (μm)	MRR (mg/min)	TWR (mg/min)	Surface roughness (μm)	D-positive	D-negative	Accessment value	Rank
0.1199	0.11157	0.11291	0.03957	0.03682	0.03839	0.117271631	0.056450115	0.67505	5
0.05354	0.26189	0.12902	0.01767	0.08642	0.04387	0.10699767	0.092552134	0.5362	19
0.15386	0.21246	0.22418	0.05077	0.07011	0.07622	0.073054442	0.105253284	0.40971	26
0.21001	0.26481	0.28011	0.0693	0.08739	0.09524	0.044533921	0.136459488	0.24605	32
0.18966	0.30605	0.17749	0.06259	0.101	0.06035	0.058846878	0.125328922	0.31951	30
0.19113	0.19894	0.08225	0.06307	0.06565	0.02797	0.094926739	0.088202181	0.51836	20
0.21539	0.099	0.10651	0.07108	0.03267	0.03621	0.107145522	0.076856782	0.58231	12
0.27215	0.2255	0.09441	0.08981	0.07441	0.0321	0.078267866	0.113691088	0.40773	27
0.22116	0.01447	0.22109	0.07298	0.00478	0.07517	0.11512605	0.092870605	0.5535	15
0.16954	0.20067	0.27106	0.05595	0.06622	0.09216	0.068435923	0.115644263	0.37177	29
0.14033	0.00203	0.22265	0.04631	0.00067	0.0757	0.128831103	0.076203257	0.62834	6
0.14111	0.12141	0.1328	0.04657	0.04006	0.04515	0.107820655	0.066082988	0.62	7
0.10118	0.14093	0.1963	0.03339	0.04651	0.06674	0.103104204	0.077157048	0.57197	14
0.24947	0.2309	0.03659	0.08233	0.0762	0.01244	0.096366091	0.107483112	0.47273	21
0.15479	0.0278	0.13929	0.05108	0.00917	0.04736	0.127731077	0.058572297	0.68561	3
0.32079	0.09571	0.28971	0.10586	0.03158	0.0985	0.081027368	0.136349355	0.37275	28
0.19516	0.22747	0.13628	0.0644	0.07506	0.04634	0.076482091	0.101005403	0.43092	25
0.04792	0.12403	0.03486	0.01581	0.04093	0.01185	0.144064501	0.041477884	0.77645	1
0.16715	0.03844	0.1208	0.05516	0.01268	0.04107	0.125913007	0.058922437	0.68122	4
0.12224	0.01253	0.2707	0.04034	0.00414	0.09204	0.12689348	0.088027666	0.59042	11
0.1589	0.24867	0.13697	0.05244	0.08206	0.04657	0.080523304	0.100253612	0.44543	24
0.01777	0.34125	0.03698	0.00586	0.11261	0.01257	0.131843672	0.111952472	0.54079	18
0.10873	0.23377	0.09516	0.03588	0.07715	0.03235	0.102616392	0.084857683	0.54736	16
0.07956	0.22492	0.03269	0.02626	0.07422	0.01112	0.124283811	0.076330059	0.61952	8
0.1989	0.26536	0.22077	0.06564	0.08757	0.07506	0.052861489	0.12334375	0.3	31
0.19606	0.01157	0.20288	0.0647	0.00382	0.06898	0.120008661	0.082581885	0.59237	10
0.12295	0.04244	0.13065	0.04057	0.01401	0.04442	0.130037263	0.049920733	0.7226	2
0.25341	0.13057	0.15008	0.08362	0.04309	0.05103	0.087073113	0.097155019	0.47264	22
0.19067	0.10948	0.26074	0.06292	0.03613	0.08865	0.08826448	0.10258889	0.46247	23
0.15648	0.12331	0.18588	0.05164	0.04069	0.0632	0.096739333	0.080062546	0.54716	17
0.13665	0.03113	0.21763	0.04509	0.01027	0.074	0.121517372	0.07473374	0.61919	9
0.20393	0.04033	0.18248	0.0673	0.01331	0.06204	0.112592846	0.080791928	0.58222	13

Table 5: Sensitivity analysis and validectory of results.

Max	2.812236	0.029483	14.66625	0.866997
Min	0.70141	0.01219	4.44156	0.569453
Mean	1.01563	0.007278	4.597194	0.726892
Std	0.514458	0.00611	2.654605	0.045471

When the gap distance was maintained at 2 mm, machined surface with minimum Ra was attained and it increases with further increase in gap distance.

The interaction impact of various input variables on the Ra of the titanium alloy is shown in Figure 7. Regardless of the process parameters, when machined at negative polarity, the samples exhibit 150% better Ra value due to the uniform heat distribution. The ideal powder concentration to attain best Ra ranges between 5 g/l to 10 g/l and exceeds beyond the limit; it leads to the densification of machined debris results in reduction of Ra. Tuning the powder concentration and gap distance to the higher parametric levels results in worsening of surface quality.

3.2. TOPSIS. The TOPSIS technique was applied to choose the best from the available option. The streamlining method starts with the arrangement of the choice network; for the ongoing exploratory run, a choice framework of 32×4 is shaped as displayed in Table 3. The standardization of the choice network was determined as per the following equation:

$$\text{Aij} = \frac{\text{Yij}}{\sum_{i=1}^{n} \sqrt{(Yij)^2}}. \tag{3}$$

$$\text{Bij} = wj * \text{Aij}. \tag{4}$$

The subsequent stage was the arrangement of a weighted standardized choice grid, as displayed in condition (4), from which the Eigen values ($\square^+$, $\square^-$)were formed where the weight (wj) of the MRR, TWR, and Ra are 0.33, 0.33, and 0.34, respectively. For beneficiary ascribed, $\square^+$ and $\square^+$ are most extreme and least upsides of weighted standardized choice framework as well as the other way around for nonbeneficiary credits, as displayed in condition (5) and (6).

For beneficiaries,

$$\blacklozenge^{+} = \text{Max (Bij)}_{i=1}^{n}, \quad \blacklozenge^{-} = \text{Min (Wij)}_{i=1}^{n}. \tag{5}$$

For nonbeneficiaries,

$$\text{\textdiamond}^{+} = \text{Min } (\text{Bij})_{i=1}^{n}, \quad \text{\textdiamond}^{-} = \text{Max } (\text{Bij})_{i=1}^{n}. \tag{6}$$

The ideal (P^+) and nonideal (P^-) arrangements are determined utilizing condition (7). The scatterings between the standards and the nonstandards by the equivalent Euclidean distances as shown in the situations 8 and its qualities are depicted in Table 4.

$$\begin{aligned} (P^+, P^-) &= \sum_{j=1}^{n} \sqrt{\left(\text{Bij} - \text{\textdiamond}^{+}\right)^2 + \left(\text{Bij} - \text{\textdiamond}^{n}\right)^2}, \\ D^i &= \left(\frac{P^-}{(P^+ + P^-)}\right). \end{aligned} \tag{7}$$

In view of the overall closeness esteem, the best blend of trial was discharge current of 10 A and gap distance of 3 mm, with the negative polarity under unmixed dielectric medium. The sensitivity analysis was conducted, and it was found that the optimal value results in highest assessment value, as depicted in Table 5.

4. Conclusion

(1) The MRR increases with the incorporation of Al_2O_3 particles, owing to the bridging effect, and positive polarity proffers high MRR, owing to the formation of the secondary electrons. Due to the increase in spark gap, machined debris were completely flushed away, which results in improvement of MRR.

(2) The most impact input variables of TWR were gap distance, as PMEDM change of polarity has no impact on TWR. At lower parametric value of gap distance, 100% raise in TWR with change in polarity was observed.

(3) Addition of particles reduces Ra accredited to the fact complete flushing of machined debris. Because of the increased thermal energy, the materials removed from the cathodes were completely flushed away, eliminating the need for the development of a remelted layer.

(4) The TOPSIS technique was utilised for the obtaining optimal solution, with the aid of mathematical modelling, the predicted results were obtained, and the optimal results were validated using the sensitivity analysis.

Data Availability

All the data are included within the manuscript.

Conflicts of Interest

The authors declare that they have no conflicts of interest.

References

[1] P. Gangidi, "A systematic approach to root cause analysis using 3 × 5 why's technique," *International Journal of Lean Six Sigma*, 2018.

[2] Y. Nagaraj, N. Jagannatha, and N. Sathisha, "Hybrid non-conventional machining of glass - a review," *Applied Mechanics and Materials*, vol. 895, pp. 8–14, 2019.

[3] R. Muhammad, M. S. Hussain, A. Maurotto, C. Siemers, A. Roy, and V. V. Silberschmidt, "Analysis of a free machining $\alpha+\beta$ titanium alloy using conventional and ultrasonically assisted turning," *Journal of Materials Processing Technology*, vol. 214, no. 4, pp. 906–915, 2014.

[4] S. Gürgen and M. A. Sofuoğlu, "Advancements in conventional machining: a case of vibration and heat-assisted machining of aerospace alloys," in *Advanced Machining and Finishing*, pp. 143–175, Elsevier, Amsterdam, Netherlands, 2021.

[5] S. Vigneshwaran, K. M. John, R. Deepak Joel Johnson, M. Uthayakumar, V. Arumugaprabu, and S. T. Kumaran, "Conventional and unconventional machining performance of natural fibre-reinforced polymer composites: a review," *Journal of Reinforced Plastics and Composites*, vol. 40, no. 15-16, pp. 553–567, 2021.

[6] R. Ranjith, P. K. Giridharan, and J. Devaraj, "Influence of titanium-coated (b4c + sic) particles on electric discharge machining of aa7050 hybrid composites," *High Temperature Material Processes An International Quarterly of High-Technology Plasma Processes*, vol. 20, no. 2, pp. 93–105, 2016.

[7] P. Kuppan, A. Rajadurai, and S. Narayanan, "Influence of EDM process parameters in deep hole drilling of Inconel 718," *International Journal of Advanced Manufacturing Technology*, vol. 38, no. 1-2, pp. 74–84, 2008.

[8] N. Pragadish and M. Pradeep Kumar, "Optimization of dry EDM process parameters using grey relational analysis," *Arabian Journal for Science and Engineering*, vol. 41, no. 11, pp. 4383–4390, 2016.

[9] M. Patel Gowdru Chandrashekarappa, S. Kumar, J. JagadishJagadish, K. Pimenov, and K. Giasin, "Experimental analysis and optimization of EDM parameters on HcHcr steel in Context with different electrodes and dielectric fluids using hybrid Taguchi-based PCA-utility and Critic-utility approaches," *Metals*, vol. 11, no. 3, 419 pages, 2021.

[10] D. H. Yoo and C. G. Song, "Inundation accident analysis using hydrodynamic model and consideration of disaster roots using cause and effect diagram," *Journal of Convergence for Information Technology*, vol. 10, no. 10, pp. 128–134, 2020.

[11] D. D. Shinde, S. Ahirrao, and R. Prasad, "Fishbone diagram: application to identify the root causes of student-staff problems in technical education," *Wireless Personal Communications*, vol. 100, no. 2, pp. 653–664, 2018.

[12] M. F. Suárez-Barraza and F. G. Rodríguez-González, "Cornerstone Root Causes through the Analysis of the Ishikawa Diagram, Is it Possible to Find Them? A First Research Approach," *International Journal of Quality and Service Sciences*, 2018.

[13] R. Ranjith, M. Prabhakar, P. K. Giridharan, and M. Ramu, "Influence of Al203 particle mixed dielectric fluid on machining performance of Ti6Al4V," *Surface Topography: Metrology and Properties*, vol. 9, no. 4, Article ID 045052, 2021.

[14] T. T. Hong, N. V. Cuong, B. T. Danh et al., "Multi-objective optimization of PMEDM process of 90CrSi alloy steel for minimum electrode wear rate and maximum material removal rate with silicon carbide powder," *Materials Science Forum*, vol. 1018, pp. 51–58, 2021.

[15] M. Prabhakar, R. Ranjith, and S. Venkatesan, "Characterization of electric discharge machining of titanium alloy utilizing MEIOT technique for orthopedic implants," *Materials Research Express*, vol. 8, no. 8, Article ID 086505, 2021.

[16] S. Mohanty, A. K. Das, and A. R. Dixit, "Surface integrity of tribo-adaptive layer prepared on Ti6Al4V through μEDC process," *Surface and Coatings Technology*, vol. 429, Article ID 127922, 2022.

[17] S. Jeavudeen, H. S. JailaniJailani, and M. Murugan, "Enhancement of machinability of titanium alloy in the Eductor based PMEDM process," *SN Applied Sciences*, vol. 3, no. 4, 490 pages, 2021.

[18] T. T. Hong, N. H. Linh, N. V. Cuong et al., "Effect of process parameters on machining time in PMEDM cylindrical shaped parts with silicon carbide powder suspended dielectric," *Materials Science Forum*, vol. 1018, pp. 97–102, 2021.

[19] C. Somu, R. Ranjith, P. K. Giridharan, and M. Ramu, "A novel Cu-Gr composite electrode development for electric discharge machining of Inconel 718 alloy," *Surface Topography: Metrology and Properties*, vol. 9, no. 3, Article ID 035025, 2021.

[20] P. K. Rout and P. C. Jena, "A review of current researches on powder mixed electrical discharge machining (PMEDM) technology," *Lecture Notes in Mechanical Engineering*, pp. 489–497, 2021.

[21] R. Ranjith and S. N. Vimalkumar, "Integrated MOORA-ELECTRE approach for solving multi-criteria decision problem," *World Journal of Engineering*, vol. 19, no. 4, pp. 510–521, 2021.

[22] S. M. Shaaban and Y. I. Mesalam, "SVC parameters optimization using a novel integrated MCDM approach," *Symmetry*, vol. 14, no. 4, 702 pages, 2022.

[23] G. Poongavanam, V. Sivalingam, R. Prabakaran, M. Salman, and S. C. Kim, "Selection of the best refrigerant for replacing R134a in automobile air conditioning system using different MCDM methods: a comparative study," *Case Studies in Thermal Engineering*, vol. 27, Article ID 101344, 2021.

[24] A. Maji, T. Deshamukhya, G. Choubey, and A. Choubey, "Performance evaluation of perforated pin fin heat sink using particle swarm optimization and MCDM techniques," *Journal of Thermal Analysis and Calorimetry*, vol. 147, no. 8, pp. 5133–5150, 2022.

[25] E. Pujiyulianto, "Effect of pulse current in manufacturing of cardiovascular stent using EDM die-sinking," *International Journal of Advanced Manufacturing Technology*, vol. 112, no. 11-12, pp. 3031–3039, 2021.

[26] L. Jiang and M. Kunieda, "High rising speed discharge current pulse for EDM generated by inductive boosting voltage circuit," *CIRP Annals*, vol. 70, no. 1, pp. 147–150, 2021.

[27] S. Lakra and R. C. Francis, "A technique of tool manufacturing by changing the polarity of EDM," *International Journal*, vol. 9, no. 5, 2021.

[28] J. Sahu, S. Shrivastava, C. Mohanty, S. Mishra, and T. K. Mahanta, "Effect of polarity on MRR and TWR in electric discharge machining," in *Advances in Mechanical Processing and Design*, pp. 543–550, Springer, Singapore, 2021.

[29] K. Ishfaq, M. A. Maqsood, S. Anwar, M. Harris, A. Alfaify, and A. W. Zia, "EDM of Ti6Al4V under nano-graphene mixed dielectric: a detailed roughness analysis," *International Journal of Advanced Manufacturing Technology*, vol. 120, no. 11-12, pp. 7375–7388, 2022.

[30] J. Lei, X. Wu, Z. Zhou, B. Xu, L. Zhu, and Y. Tang, "Sustainable mass production of blind multi-microgrooves by EDM with a long-laminated electrode," *Journal of Cleaner Production*, vol. 279, Article ID 123492, 2021.

[31] B. Xu, M. Q. Lian, S. G. Chen et al., "Combining PMEDM with the tool electrode sloshing to reduce recast layer of titanium alloy generated from EDM," *International Journal of Advanced Manufacturing Technology*, vol. 117, no. 5-6, pp. 1535–1545, 2021.